J Intell Robot Syst (2010) 60:341–363
DOI 10.1007/s10846-010-9423-x

Dynamic Load Carrying Capacity of Flexible Cable Suspended Robot: Robust Feedback Linearization Control Approach

Moharam Habibnejad Korayem · H. Tourajizadeh · M. Bamdad

Received: 14 November 2009 / Accepted: 5 April 2010 / Published online: 5 May 2010

Abstract In this paper dynamic load carrying capacity (DLCC) of a cable robot equipped with a closed loop control system based on feedback linearization, is calculated for both rigid and flexible joint systems. This parameter is the most important character of a cable robot since the main application of this kind of robots is their high load carrying capacity. First of all the dynamic equations required for control approach are represented and then the formulation of control approach is driven based on feedback linearization method which is the most suitable control algorithm for nonlinear dynamic systems like robots. This method provides a perfect accuracy and also satisfies the Lyapunov stability since any desired pole placement can be achieved by using suitable gain for controller. Flexible joint cable robot is also analyzed in this paper and its stability is ensured by implementing robust control for the designed control system. DLCC of the robot is calculated considering motor torque constrain and accuracy constrain. Finally a simulation study is done for two samples of rigid cable robot, a planar complete constrained sample with three cables and 2 degrees of freedom and a spatial unconstrained case with six cables and 6 degrees of freedom. Simulation studies continue with the same spatial robot but flexible joint characteristics. Not only the DLCC of the mentioned robots are calculated but also required motors torque and desired angular velocity of the motors are calculated in the closed loop condition for a predefined trajectory. The effectiveness of the designed controller is shown by the aid of simulation results as well as comparison between rigid and flexible systems.

Keywords Cable suspended robot · Flexible joint · Robust feedback linearization · Control · Dynamic load carrying capacity

M. H. Korayem (✉) · H. Tourajizadeh · M. Bamdad
Robotic Research Laboratory, Center of Excellence in Experimental Solid Mechanics and Dynamics, College of Mechanical Engineering, Iran University of Science and Technology, Tehran, Iran
e-mail: hkorayem@iust.ac.ir

1 Introduction

New generation of manipulators as cable robots, are widely applicable today, because of their lightness, easy assembling capability and sufficient accuracy for many applications such as cranes, rescue robots, studio cams, industrial handling equipments, welding instruments and etc [1]. There is a fundamental difference between dynamic applications of cable robots and linkage robots. Against the linkage robots, the cable robots are restricted in just tensional forces to move the end-effector since cables cannot bear compression. Although all of the researches of this paper are limited to allowable workspace in which there is no negative tension in cables, this limitation makes the control procedure more challengeable. This complexity seems more critical in the case of flexible system in which uncertainties can affect on the calculated results. Because of nonlinear nature of dynamic equation of cable robots [2–4], a proper control method is needed to simplify the complicacy of nonlinearities. In order to achieve this goal, one of the most suitable methods which has been developed is feedback linearization approach [5–8] in which the control input of the outer closed loop is defined by the feedback states in the way that leads the system to linear dynamic equations for the inner closed loop of the system. Choosing the feedback linearization method not only provides a good accuracy for the system by converting it to a simple PID control, but also Lyapunov stability of the system is ensured by choosing proper gains for the controller to achieve a good pole placement. Moreover, in practical experiments, we are not permitted to suppose rigidity for all parts of the robot, while elasticity at two important parts of the plant, joints and cables, can make considerable effects on the dynamic of the system. By rigidity we mean that there is no clearance or elasticity between the actuator and the pulleys whereas a kind of angular spring is needed to add to the joints in order to model the joint flexibility. In flexible case in which some states remain uncontrolled, parametric uncertainties and vibrational disturbances of the joints are compensated by the aid of adding robust control to the designed control system. Flexible joint robots are studied in [9, 10] and vibration analysis of elastic cable robots is done in [11, 12]. A workspace study of these kinds of robots is also done in [13]. A different method to control a flexible cable robot is presented in [14] using active boundary control algorithm.

To sum up due to high capacity of load carrying of these robots and the importance of this character in defining the application of a designed robot, the main purpose of this paper is calculating the DLCC of a closed loop cable robot especially with flexible joints and comparing it with the rigid system results. In [5] DLCC is defined for flexible joint robots and in [6] this parameter is calculated for a mobile based robot. It is also calculated for open-loop cable robot in [17]. Iteration method is used in order to calculate the DLCC of the closed loop cable robot considering allowable motor torque and allowable error bounds [5]. It is obvious that equipping the end-effector with a controller for a predefined trajectory causes an effective reduction on its undesired vibrations and improves its accuracy and so its DLCC. First the dynamic equations required for control procedure are represented. The dynamic equations of spatial cable robot with elastic joints are driven by coupling the vibration equations of the joints with dynamic equations of the end-effector, then feedback linearization algorithm together with robust method are imposed on the case of study and its controllability effectiveness is approved by the aid of some simulations. Required

motor torque and desired angular velocity of the motors are calculated for moving the end-effector within a predefined trajectory. DLCC of the robot for both rigid and flexible joint cases are calculated and are compared together. Finally all of these steps are supported by performing some simulations which prove the effectiveness of the designed controller and illustrate the DLCC differences of rigid and flexible joints robots.

2 Dynamical Modelling

2.1 Planar Dynamics

Consider a planar cable robot with a concentrated mass with three cables and 2 degrees of freedom, x, y as is depicted in Fig. 1. It is shown in [2] that required tension for each cable and dynamic equation of such system can be explained by:

$$T = 1/r\left(\tau - J\left(d/dT\left(\partial\beta/\partial X\right)\dot{X} + \ddot{X}\left(\partial\beta/\partial X\right)\right) - C\left(\partial\beta/\partial X\right)\dot{X}\right) \tag{1}$$

$$M_{eq}(X)\ddot{X} + N\left(X, \dot{X}\right) = S(X)\tau;$$
$$where \qquad S = \begin{bmatrix} -\cos\Theta_1 & -\cos\Theta_2 & -\cos\Theta_3 \\ -\sin\Theta_1 & -\sin\Theta_2 & -\sin\Theta_3 \end{bmatrix};$$
$$M_{eq} = rm + S(X)J\left(\partial\beta/\partial X\right); N\left(X, \dot{X}\right) = S(X)\left(J\frac{d}{dt}\left(\partial\beta/\partial X\right) + C\left(\partial\beta/\partial X\right)\right)\dot{X} \tag{2}$$

where T is the tension of the cables, τ is the torque exerted by the motors, r is the radius of the pulleys, β is the angle of the pulleys, c is the damping coefficient of the motors, J is the rotary inertia of the pulleys, S is the Jacobean matrix and Θ is the angle of the cables.

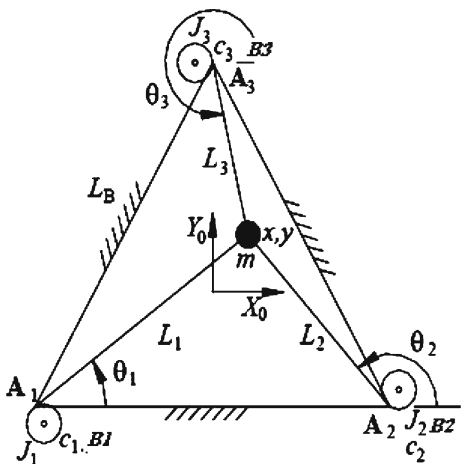

Fig. 1 Planar model of cable robot [2]

2.2 Spatial Dynamics

For the spatial case, suppose a triangular shape end-effector like Fig. 2 which is suspended through six cables and has 6 degrees of freedom, x, y, z, ψ, Θ, φ. It is provable that the tension of the cables and its dynamic equation can be shown as below [4]:

$$T = 1/r\left(\tau - J\left(d/dT\left(\partial\beta/\partial X\right)\dot{X} + \ddot{X}\left(\partial\beta/\partial X\right)\right) - C\left(\partial\beta/\partial X\right)\dot{X}\right)$$
$$D\left(X\right)\ddot{X} + C\left(X, \dot{X}\right)\dot{X} + g\left(X\right) = -S^{T}\left(q\left(X\right)\right)T; \tag{3}$$

where $q(X)$ is the length of the cables and:

$$D = \begin{bmatrix} mI_3 & 0 \\ 0 & P^T I P \end{bmatrix}; C = \begin{bmatrix} 0_3 \\ P^T\left\{I\dot{P}\dot{o} + (P\dot{o}) \times I\left(Po\right)\right\} \end{bmatrix}; g = \begin{bmatrix} 0 \\ 0 \\ -mg \\ 0_3 \end{bmatrix};$$

$$S = \left[\frac{\partial q_i}{\partial x_j}\right]_{i\times j}; P = \begin{bmatrix} 1 & 0 & -sin\theta \\ 0 & cos\,\psi & sin\,\psi\, cos\,\Theta \\ 0 & -sin\,\psi & cos\,\psi\, cos\,\Theta \end{bmatrix}; \dot{o} = \begin{bmatrix} \dot{\psi} \\ \dot{\Theta} \\ \dot{\varphi} \end{bmatrix}; X = \{x, y, z, x, y, z, \psi, \Theta, \varphi\}$$

2.3 Flexible Joint Dynamics

Existence of clearance or elasticity between actuators and pulleys can affect the presented dynamics. The elasticity can be modeled by an angular spring between the motors and the pulleys (Fig. 3).

It is obvious that in this case motors rotate with a different angular velocity in comparison to the pulleys, however they are dependent on each other with a kind

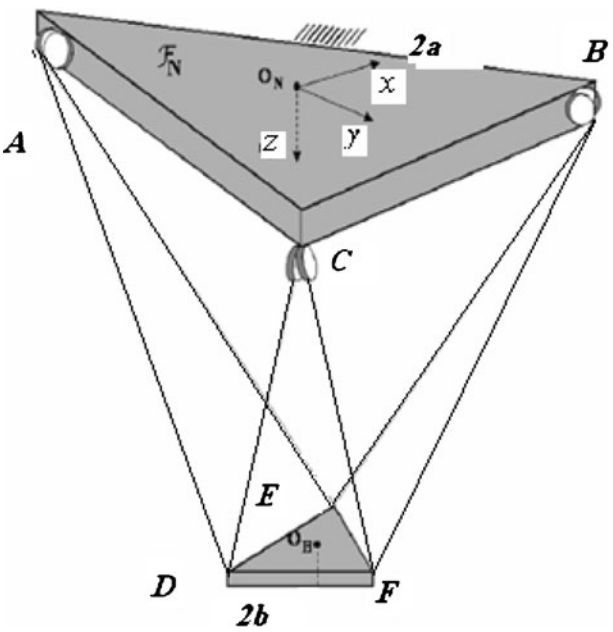

Fig. 2 Spatial model of cable robot [4]

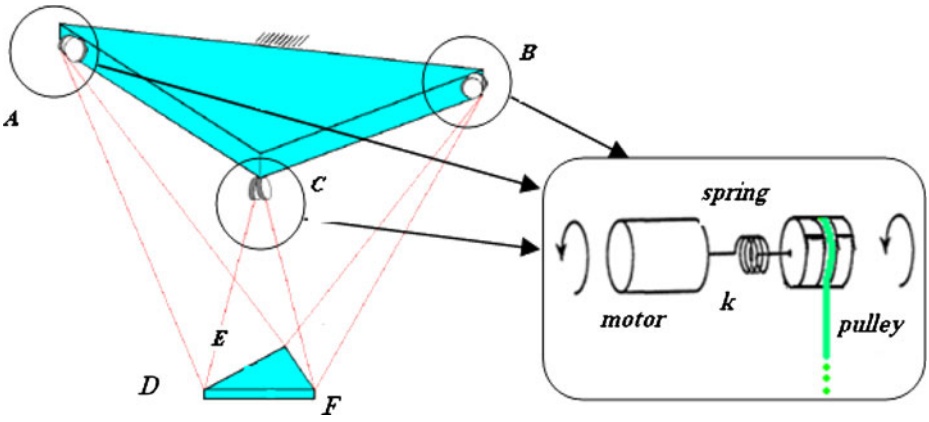

Fig. 3 Modeling of elastic joint for cable robot

of non-holonomic constraint. Using Newton-Euler or Lagrange approach, it can be written [5]:

$$\begin{aligned} J_i\ddot{\beta}_i + K_i\left(\beta_i - \beta_i'\right) &= -r_i T_i \\ J_i'\ddot{\beta}_i' - K_i\left(\beta_i - \beta_i'\right) &= \tau_i \end{aligned} \tag{4}$$

The first equation indicates the dynamic of the pulleys and the second shows motor's dynamic, where J, B are in turn the rotary inertia and angle of the pulleys, J', β'' are the same variables for motor, K is the elasticity coefficient of the spring between the motor and the pulley, r is the radius of the pulleys, T is the tension applied to the cables and τ is the torque produced by the motors. Combining these two last equations leads to:

$$J_i\ddot{\beta}_i + J_i'\ddot{\beta}_i' = \tau_i - r_i T_i \tag{5}$$

The relation between the angle of the pulleys and the position of the end-effector can be written as below [3]:

$$\begin{aligned} \dot{\beta} &= \frac{\partial \beta}{\partial X}\dot{X} \\ \ddot{\beta} &= d/dt\left(\partial\beta/\partial X\right)\dot{X} + \ddot{X}\left(\partial\beta/\partial X\right) \end{aligned} \tag{6}$$

According to these two last equations we have:

$$T = \frac{1}{r}\left(\tau - J'\ddot{\beta}' - J\left(\frac{d}{dt}\left(\frac{\partial\beta}{\partial X}\right)\dot{X}\right) + \frac{\partial\beta}{\partial X}\ddot{X}\right)\Bigg) \tag{7}$$

Dynamic of the end-effector can be defined by Eq. 3 where T is replaced by the tension that is just calculated in this case. Equation 7 illustrates the required amount of tension should be applied to the cables to achieve the desired position of the end-effector and can be used in control procedure. So the dynamic of the system can be explained by 12 degrees of freedom, 6 for end-effector (X) and 6 for motors angle (β'), while the pulleys angle (β) can be driven by X:

$$Z = \left\{x, y, z, \Psi, \Theta, \varphi, \beta_1', \beta_2', \beta_3', \beta_4', \beta_5', \beta_6'\right\} \tag{8}$$

3 Control Scheme

Control algorithm used in this paper is feedback linearization method. Converting the nonlinear dynamic equations into linear one by imposing the control inputs causes it to be the most efficient control algorithm for nonlinear systems. It makes it possible to achieve a simple PID controlled system out of a non linear system in which not only Lyapunov stability is satisfied but also any desired tracking accuracy is possible by choosing suitable gains for the controller. Robust control is also attached in the case of flexible joints system to cancel uncertainty effects. In this method, state spaces that are composed of degrees of freedom of manipulator are fed back to the controller and based on them input of the outer loop controller is defined so that the equations of the state space convert to a linear form. Finally the inputs of inner loop which are the torques of the motors (Fig. 4) are calculated as the required torque that should be applied to the system to have a sufficient accuracy of tracking for a predefined trajectory [5].

3.1 Planar Control Scheme

Considering 2 degrees of freedom for a planar cable robot as was mentioned in the previous section, state space can be developed as below:

$$\begin{cases} z_1 = x \\ z_2 = \dot{x} \\ z_3 = y \\ z_4 = \dot{y} \end{cases} \Rightarrow \begin{cases} \dot{z}_1 = z_2 \\ \dot{z}_2 = \dfrac{1}{M_{eq}(X)} \left(-N\left(X, \dot{X}\right) + S(X)\,\tau\right)_1 \\ \dot{z}_3 = z_4 \\ \dot{z}_4 = \dfrac{1}{M_{eq}(X)} \left(-N\left(X, \dot{X}\right) + S(X)\,\tau\right)_2 \end{cases} \tag{9}$$

It can be seen that non-linear terms appear just in those states which involve control input (motors torque), and so it is possible to impose feedback linearization method

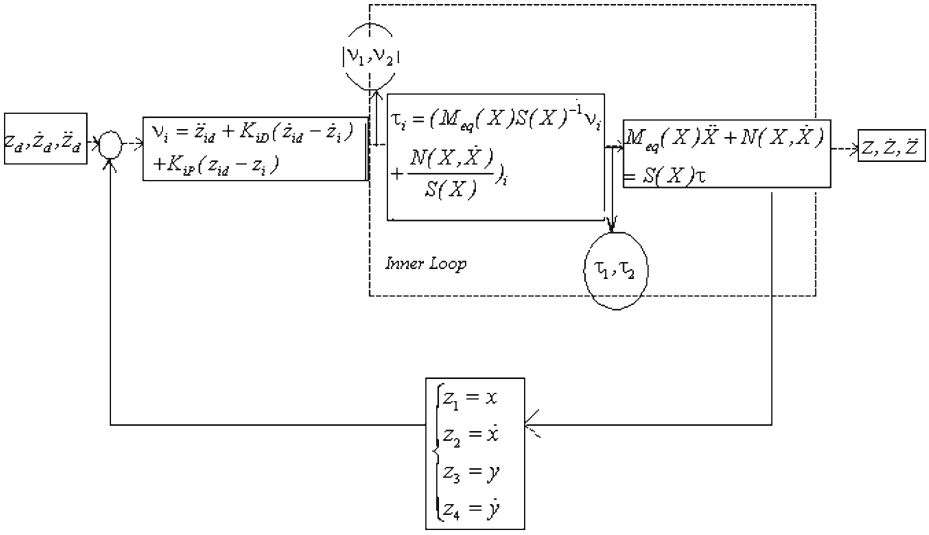

Fig. 4 Closed loop model of feedback linearization controller

on this state space without using similarity transformation. To achieve this goal outer loop input v is set as the acceleration of the system's degrees of freedom. So the required torque that should be exerted by the motors according to the Eq. 9 becomes:

$$\begin{cases} \tau_1 = \left(M_{eq}(X)\, S(X)^{-1}\, \nu_1 + \frac{N(X,\dot{X})}{S(X)} \right)_1 \\ \tau_2 = \left(M_{eq}(X)\, S(X)^{-1}\, \nu_2 + \frac{N(X,\dot{X})}{S(X)} \right)_2 \end{cases} \tag{10}$$

It should be considered that here there is a 2 degrees of freedom system but three controller inputs, so two of required motors torque can be definitely defined according to the feedback linearization method while the third one should be determined in the way that results in positive tension for all of three cables. According to a proposed algorithm explained by [7, 15] motors torque can be obtained by Eq. 11:

$$S^{*}\tau = S\tau \Rightarrow \tau = [S]^{T} \left([A][A]^{T} \right)^{-1} \{S\tau\} + \alpha \{N\} \tag{11}$$

where N is the null vector of matrix S. Based on the control law, $S\tau$ and S are defined from dynamic analysis. By imposing these inner loop inputs on the system, following state space can be achieved that is completely linear:

$$\begin{cases} \dot{z}_1 = z_2, \dot{z}_2 = \nu_1 \\ \dot{z}_3 = z_4, \dot{z}_4 = \nu_2 \end{cases} \tag{12}$$

Following values are chosen for the outer loop input (v) to achieve a simple PID controlled system:

$$\begin{cases} \nu_1 = \ddot{z}_{1d} + K_{1D}(\dot{z}_{1d} - \dot{z}_1) + K_{1P}(z_{1d} - z_1) \\ \nu_2 = \ddot{z}_{3d} + K_{2D}(\dot{z}_{3d} - \dot{z}_3) + K_{2P}(z_{3d} - z_3) \end{cases} \tag{13}$$

where $z_d, \dot{z}_d, \ddot{z}_d$ are in turn desired position, velocity and acceleration based on predefined trajectory and K_P, K_D are controller gains that should be determined according to required accuracy, so substituting Eq. 13 into Eq. 12 results in dynamic error equations as below:

$$\begin{cases} \ddot{e}_1 + K_{1D}\dot{e}_1 + K_{1P}e_1 = 0 \\ \ddot{e}_2 + K_{2D}\dot{e}_2 + K_{2P}e_2 = 0 \end{cases} \Rightarrow \begin{cases} \lambda_{1,2} = 1/2\left(-K_{1D} +/- \sqrt{{K_{1D}}^2 - 4K_{1P}} \right) \\ \lambda_{3,4} = 1/2\left(-K_{2D} +/- \sqrt{{K_{2D}}^2 - 4K_{2P}} \right) \end{cases} \tag{14}$$

where e_1, e_2 in turn are the errors of x, y and λ_1, λ_2 are the poles of dynamic behavior of the system, which can be placed wherever is desired by calibrating the gains of the controller.

3.2 Spatial Control Scheme

In a similar way according to Eq. 3 the state space of a spatial robot can be driven:

$$\begin{cases} z_1 = x; z_2 = \dot{x}; z_3 = y \\ z_4 = \dot{y}; z_5 = z; z_6 = \dot{z} \\ z_7 = \psi; z_8 = \dot{\psi}; z_9 = \theta \\ z_{10} = \dot{\theta}; z_{11} = \varphi; z_{12} = \dot{\varphi} \end{cases} \Rightarrow \begin{cases} \dot{z}_i = z_{(i+1)}; if: i = odd; i = 1, ..., 12 \\ \dot{z}_i = \dfrac{1}{D}\left(-C\dot{X} - g + S^T T \right)_{i/2}; if: else \end{cases} \tag{15}$$

Similar to the planar case the state space terms and inputs are so that feedback linearization method can be applied, v is set as the acceleration of the system and so cables tension and motors torque of the system are calculated as below:

$$T_i = \left\{S^{-T}\left(Dv + C\dot{X} + g\right)\right\}_i \Rightarrow \tau_i = rS^{-T}\left(Dv + C\dot{X} + g\right) + J\ddot{\beta} + C\dot{\beta}; i = 1, ., 6 \tag{16}$$

By imposing these values on the inner loop inputs again the following linear state space can be achieved:

$$\begin{cases} \dot{z}_i = z_{(i+1)}; if : i = odd; i = 1, ..., 12 \\ \dot{z}_i = v; if : else \end{cases} \tag{17}$$

Choosing the following values for the outer loop inputs (v):

$$v_i = \ddot{z}_{(2i-1)d} + K_{iD}\left(\dot{z}_{(2i-1)d} - \dot{z}_{(2i-1)}\right) + K_{iP}\left(z_{(2i-1)d} - z_{(2i-1)}\right); i = 1, .., 6 \tag{18}$$

And substituting Eq. 18 into Eq. 17 result in the following dynamic error equations:

$$\ddot{e}_i + K_{iD}\dot{e}_i + K_{iP}e_i = 0 \Rightarrow \left(\lambda_{1,2}\right)_i = 1/2\left(-K_{iD} + / - \sqrt{K_{iD}^2 - 4K_{iP}}\right) \tag{19}$$

Again the poles can be placed wherever is desired by calibrating the controller gains.

3.3 Flexible Joint Control Scheme

According to Eq. 8, the state space variables can be defined as:

$$z = \left\{X, \dot{X}, \beta', \dot{\beta}'\right\} \tag{20}$$

where X is the position and orientation vector of the end-effector and β' is the angle vector of the motors. Substituting Eq. 7 into Eq. 15 makes it possible to formulate the state space of flexible case.

$$\begin{cases} if : i = odd : \\ \dot{z}_i = z_{i+1} \\ if : i = even, i \le 12 : \\ \dot{z}_i = \left\{ \dfrac{1}{D + \left(S^T J/r\right)\left(\dfrac{\partial\beta}{\partial X}\right)} \left(-C\dot{X} - g - S^T\left(\dfrac{1}{r}\left(\tau - J'\ddot{\beta}' - J\left(\dfrac{d}{dt}\left(\dfrac{\partial\beta}{\partial X}\right)\dot{X}\right)\right)\right)\right) \right\}_i \\ if : i = even, i > 12 : \\ \dot{z}_i = \left\{\dfrac{1}{J'}\left(\tau + K\left(\beta - \beta'\right)\right)\right\}_i \end{cases} \tag{21}$$

It can be seen that all of the nonlinear terms related to the main system (first 12 equations) in this state space contain control input and so this state space is suitable to be used for feedback linearization method because all of the non linear terms can be converted into linear one by choosing suitable input motors torque [16]. On the other hand although the equations related to motor's degrees of freedom do not contain control input, they are not nonlinear and there is no need for them to

be controlled under feedback linearization controller, so they should just remain stable under applied motors torque produced by feedback linearization algorithm. To ensure the stability of these uncontrolled states, robust control is added to this controller. Based on this strategy, the control inputs are defined as below:

$$\begin{aligned} &for, i = 1, \ldots, 6 \\ &T_i = \left(-\frac{1}{S^T} \left(D\left(X\right) v + C\left(X, \dot{X}\right) \dot{X} + g\left(X\right) \right) \right)_i \\ &\tau_i = \left(-rS^{-T} \left(Dv + C\dot{X} + g \right) + J'\ddot{\beta}' + J \left(\frac{d}{dt} \left(\frac{\partial \beta}{\partial X} \right) \dot{X} + \frac{\partial \beta}{\partial X} \ddot{X} \right) \right)_i \end{aligned} \tag{22}$$

Using these values for controlling the system, the state space is as below where the terms related to the main system are linear:

$$\begin{cases} if : i = odd : \\ \dot{z}_i = z_{i+1} \\ if : i = even, i \leq 12 : \\ \dot{z}_i = v_i \\ if : i = even, i > 12 : \\ \dot{z}_i = \left\{ \frac{1}{J'} \left(\tau + K\left(\beta - \beta' \right) \right) \right\}_i \end{cases} \tag{23}$$

where τ can be defined by simultaneous solving of differential equations of Eq. 4 in which T is replaced by (22) and δ_{vi} are inputs of outer control loop that should be defined based on feedback linearization method. Defining them based on Eq. 18 results in error equations like Eq. 19 for the first 12 terms of state space which are related to the main system.

Now the motor dynamic (last 12 equations of the state space) should be substituted by the calculated motors torque to see if they are stable or not, according to Eqs. 22 and 23:

$$\ddot{\beta}' = \left\{ \frac{1}{1 + J'} \left(-rS^{-T} \left(Dv + C\dot{X} + g \right) + J \left(\frac{d}{dt} \left(\frac{\partial \beta}{\partial X} \right) \dot{X} + \frac{\partial \beta}{\partial X} \ddot{X} \right) + K\left(\beta - \beta' \right) \right) \right\} \tag{24}$$

that can be explained as:

$$\begin{aligned} &\ddot{\beta}' + K\beta' = H; \\ &H = \left\{ \frac{1}{1 + J'} \left(-rS^{-T} \left(Dv + C\dot{X} + g \right) + J \left(\frac{d}{dt} \left(\frac{\partial \beta}{\partial X} \right) \dot{X} + \frac{\partial \beta}{\partial X} \ddot{X} \right) + K\beta \right) \right\} \end{aligned} \tag{25}$$

Since term H is independent of β', it can be supposed as a time dependent input force, so as far as the coefficient of those terms of Fourier expansion of H which have the same frequency of the natural frequency of the system are not considerable, β' remains stable. Otherwise robust controller improves the stability of the system.

3.4 Robust Control Scheme

It is seen that according to feedback linearization method, nonlinear terms in the state space are equal to v in all of studied cases and so the following motors torque are driven:

$$i = even, i \leq 12 :$$
$$\dot{z}_i = v_i \Rightarrow \tau_i = \left[\left(-rS^{-T} D\right) v + \left(-rS^{-T} \left(C\dot{X} + g\right) + J'\ddot{\beta}' + J\left(\frac{d}{dt}\left(\frac{\partial \beta}{\partial X}\right)\dot{X} + \frac{\partial \beta}{\partial X}\ddot{X}\right)\right]_i \tag{26}$$

and it can be written as:

$$\tau_i = \alpha\left(X, \dot{X}, \beta', \dot{\beta}'\right) + \gamma(X)\, v$$
$$\alpha = \left(-rS^{-T}\left(C\dot{X} + g\right) + J'\ddot{\beta}' + J\left(\frac{d}{dt}\left(\frac{\partial \beta}{\partial X}\right)\dot{X} + \frac{\partial \beta}{\partial X}\ddot{X}\right); \gamma = -rS^{-T} D \tag{27}$$

As it was mentioned, in the case of flexible joint, the system is uncontrollable since the number of control inputs are less than the degrees of freedom of the system. So there is a risk of instability for the uncontrolled states due to existing uncertainties in the system. By the aid of a robust control system, this instability can be improved. Existence of any kind of uncertainties involving parametric or disturbance can change the above control input to the following one:

$$\tau_i = \hat{\alpha}\left(X, \dot{X}, \beta', \dot{\beta}'\right) + \hat{\gamma}(X)\, v \tag{28}$$

Substituting this value into Eq. 23 results in:

$$\dot{z}_i = v_i + \eta_i(v, z) \tag{29}$$

where:

$$\eta = \left(\gamma^{-1}\hat{\gamma} - I\right) v + \gamma^{-1}\Delta\alpha$$
$$\Delta\alpha = \hat{\alpha} - \alpha \tag{30}$$

is referred as "uncertainty". In order to achieve a linear state space which is required in feedback linearization algorithm, the following outer closed loop inputs should be applied:

$$v_i = \dot{z}_{di} - k_{1i}(z_{di} - z_i) - k_{2i}\int (z_{di} - z_i)\, dt + \Delta v_i \tag{31}$$

Substituting this value into Eq. 17 results in the following error equation:

$$\ddot{e}_i + k_{1i}\dot{e}_i + k_{2i}e_i = \psi_i + \Delta v_i \tag{32}$$

where:

$$\psi_i = \left(\gamma^{-1}\hat{\gamma} - I\right)\left(\dot{z}_{di} - k_{1i}(z_{di} - z_i) - k_{2i}\int (z_{di} - z_i)\, dt + \Delta v_i\right) + \gamma^{-1}\Delta\alpha \tag{33}$$

Using the Lyapunov's second law to ensure the stability, Δv should be chosen as [10]:

$$\Delta v = \begin{cases} -\rho \frac{B^T Pe}{\|B^T Pe\|}; if \left\| B^T Pe \right\| \neq 0 \\ 0; if \left\| B^T Pe \right\| = 0 \end{cases} \tag{34}$$

where P is the unique positive definite solution of the Lyapunov equation:

$$A^T P + PA = -Q \tag{35}$$

for a given positive definite Q. Also A, B, e and ρ should be defined as below:

$$\mathrm{A} = \begin{bmatrix} 0 & 1 & 0 & 0 & 0 & 0 & 0 & 0 & 0 & 0 & 0 & 0 \\ k_{xp} & k_{xd} & 0 & 0 & 0 & 0 & 0 & 0 & 0 & 0 & 0 & 0 \\ 0 & 0 & 0 & 1 & 0 & 0 & 0 & 0 & 0 & 0 & 0 & 0 \\ 0 & 0 & k_{yp} & k_{yd} & 0 & 0 & 0 & 0 & 0 & 0 & 0 & 0 \\ 0 & 0 & 0 & 0 & 0 & 1 & 0 & 0 & 0 & 0 & 0 & 0 \\ 0 & 0 & 0 & 0 & k_{zp} & k_{zd} & 0 & 0 & 0 & 0 & 0 & 0 \\ 0 & 0 & 0 & 0 & 0 & 0 & 0 & 1 & 0 & 0 & 0 & 0 \\ 0 & 0 & 0 & 0 & 0 & 0 & k_{\psi p} & k_{\psi d} & 0 & 0 & 0 & 0 \\ 0 & 0 & 0 & 0 & 0 & 0 & 0 & 0 & 0 & 1 & 0 & 0 \\ 0 & 0 & 0 & 0 & 0 & 0 & 0 & 0 & k_{\theta p} & k_{\theta d} & 0 & 0 \\ 0 & 0 & 0 & 0 & 0 & 0 & 0 & 0 & 0 & 0 & 0 & 1 \\ 0 & 0 & 0 & 0 & 0 & 0 & 0 & 0 & 0 & 0 & k_{\phi p} & k_{\phi d} \end{bmatrix}; B = \begin{bmatrix} 0 & 0 & 0 & 0 & 0 & 0 \\ 1 & 0 & 0 & 0 & 0 & 0 \\ 0 & 0 & 0 & 0 & 0 & 0 \\ 0 & 1 & 0 & 0 & 0 & 0 \\ 0 & 0 & 0 & 0 & 0 & 0 \\ 0 & 0 & 1 & 0 & 0 & 0 \\ 0 & 0 & 0 & 0 & 0 & 0 \\ 0 & 0 & 0 & 1 & 0 & 0 \\ 0 & 0 & 0 & 0 & 0 & 0 \\ 0 & 0 & 0 & 0 & 1 & 0 \\ 0 & 0 & 0 & 0 & 0 & 0 \\ 0 & 0 & 0 & 0 & 0 & 1 \end{bmatrix}; e = \begin{bmatrix} e_x \\ \dot{e}_x \\ e_y \\ \dot{e}_y \\ e_z \\ \dot{e}_z \\ e_\psi \\ \dot{e}_\psi \\ e_\theta \\ \dot{e}_\theta \\ e_\phi \\ \dot{e}_\phi \end{bmatrix}; \tag{36}$$

$$\rho = \frac{1}{1-\zeta} [\zeta \ (\|\dot{z}_d\| + \|-Ae\|) + \bar{\beta}\phi`$$

where k_{ip}, k_{id} are controller gains of i th degree of freedom and $\zeta < 1$, $\bar{\gamma}$ and φ should be defined according to these three assumptions:

1. Positive constants $\bar{\gamma}$ and γ exist such that:

$$\gamma \leq \left\| \gamma^{-1}(X) \right\| \leq \bar{\gamma}$$

2. There is a positive constant $\zeta < 1$ such that:

$$\left\| \gamma^{-1} \hat{\gamma} - 1 \right\| \leq \zeta$$

3. There is a known function φ(X, t) such that:

$$\left\| \hat{\alpha} - \alpha \right\| \leq \varphi < \infty$$

And finally $\hat{\alpha}$ and $\hat{\gamma}$ are defined according to the uncertainty specifications of the dynamic system.

4 Simulation of Control Procedure

4.1 Planar Simulation

Consider a planar circle with described equation in Table 1 as a predefined trajectory and planar robot characteristics of Table 2:

Motors torque, cables tension and error profiles for a closed loop system are shown in Fig. 5, it can be seen that cables tension remain positive as a cable robot is expected to be:

Table 1 Reference input for planar simulation

t <= 0.5,	0.5<t<=1
$x = 0.2165\cos(4\pi(t^2))$,	$x = 0.2165\cos\left(4\pi\left((-t+1)^2\right)\right)$,
$y = 0.2165\sin(4\pi(t^2))$	$y = -0.2165\sin\left(4\pi\left((-t+1)^2\right)\right)$

Table 2 Characteristics of planar system

Name	Symbol	Value	Unit
Control gain of velocity	K_D	*diag*[10]	
Control gain of position	K_P	*diag*[2000]	
Radius of the motor	r	*diag*[0.05]	m
Rotary inertia of the pulley	J	*diag*[0.0008]	$kg.m^2$
Mass of the end-effector	m	1	kg
Triangle side		1	m

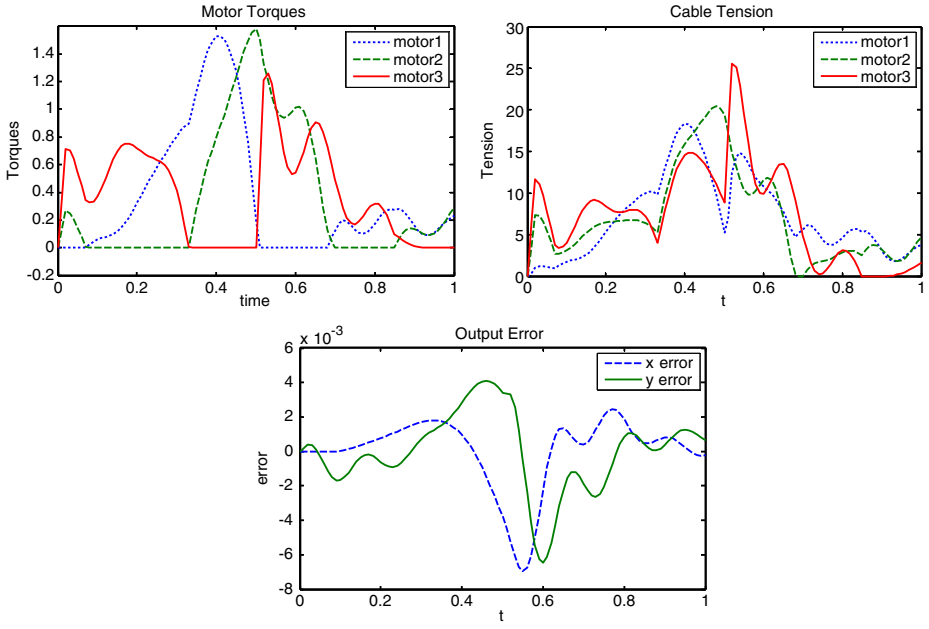

Fig. 5 Torques, tensions, and error profiles of planar simulation

4.2 Spatial Simulation

The same procedure can be done for the same input and parameters like Tables 3 and 4 [4]:

Motors torque, cables tension and error profiles for a closed loop system are shown in Fig. 6.

Table 3 Reference input for spatial simulation

$t <= 0.5$	$0.5 < t <= 1$	$z = 0.1, \psi = 0.1,$
$x = 0.1\cos(4\text{pi}(t^2)),$	$x = 0.1\cos\left(4\text{pi}\left((-t+1)^2\right)\right),$	$\Theta = 0.1, \varphi = 0.1$
$y = 0.1\sin(4\text{pi}(t^2))$	$y = -0.1\sin\left(4\text{pi}\left((-t+1)^2\right)\right)$	

Table 4 Characteristics of spatial system

Name	Symbol	Value	Unit
Moment of inertia of the end-effector triangle	I	$Ixx = Iyy = 0.58\ Izz = 1.16$	kg.m^2
Half of the base and end-effector triangle	a, b	0.47, 0.148	m
Control gain of velocity	K_D	$diag$[20]	
Control gain of position	K_P	$diag$[30]	
Radius of the motor	r	$diag$[0.05]	m
Damping coefficient	c	$diag$[0.01]	N.m/rad
Rotary inertia of the pulley	J	$diag$[0.0008]	kg.m^2
Mass of the end-effector	m	11	kg

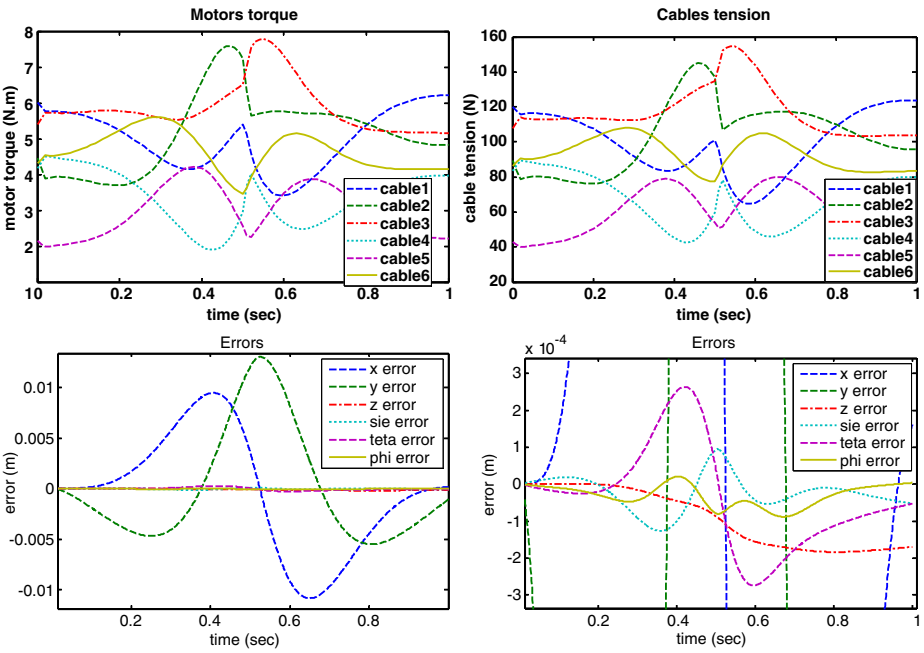

Fig. 6 Torques, tensions, and error profiles of spatial simulation

4.3 Flexible Joint Simulation

Consider a spatial cable robot which has elasticity between their motors and pulleys. For the same input of Table 3 and dynamic characteristics of Table 5:

The profiles of motors torque in comparison to rigid case are shown in Fig. 7. Vibration is considerable just during input change which occurs at the middle of the simulation.

Table 5 Characteristics of flexible joint system

Name	Symbol	Value	Unit
Moment of inertia of the end-effector triangle	I	$Ixx = Iyy = 0.58\ Izz = 1.16$	kg.m^2
Half of the base and end-effector triangle	a, b	0.47, 0.148	m
Control gain of velocity	K_D	$diag$[20]	
Control gain of position	K_P	$diag$[30]	
Radius of the motor	r	$diag$[0.05]	m
Coefficient of joint elasticity	K	$diag$[2]	$\frac{N.m}{rad}$
Rotary inertia of the motor and pulley	J', J	$diag$[0.0004]	kg.m^2
Mass of the end-effector	m	11	kg

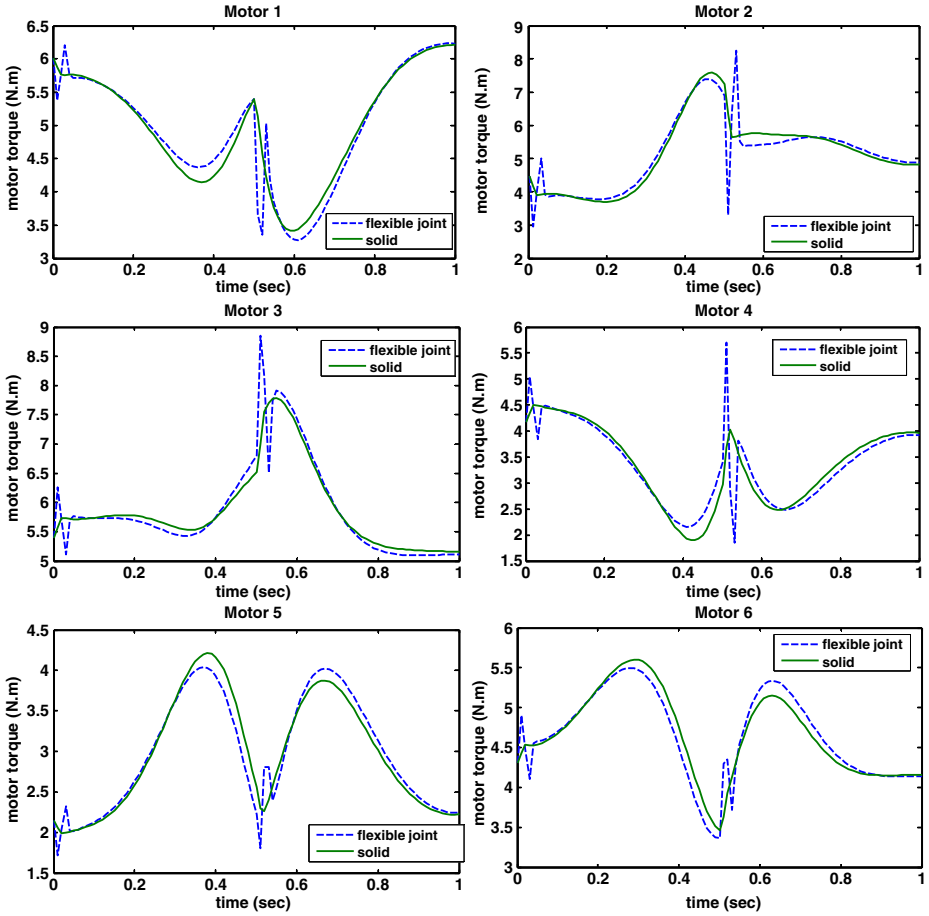

Fig. 7 Required motors torque for flexible joint robot in comparison to rigid case

4.4 Flexible Joint Simulation Considering Robust Control Context

Robust control should be considered in the case of flexible robot to avoid instability due to noises or any kind of parametric uncertainties. Therefore robust control algorithm described in the control section is attached to the simulated system considering following normal disturbances and parametric uncertainties (see Table 6).

Applying Eq. 34 results in the following control input deviation (see Fig 8).

These changes in control input and as a result in the motors torque improve tracking as it can be compared in Fig. 9:

Table 6 Uncertainties

Name	Symbol	Value	Unit
Mass uncertainty range	m	$m = \mathrm{m} \pm 0.1m$	kg
Elasticity coefficient uncertainty range	k	$k = k \pm 0.1k$	N.m/rad
External disturbance mean value	n_m	0.5	N
External disturbance variance	v	0.2	N
External disturbance uncertainty range	n	$n = n \pm 0.1n$	N

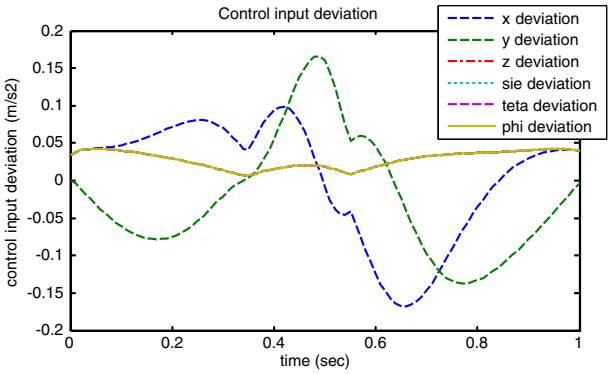

Fig. 8 Additional control input that should be applied to the uncertain system

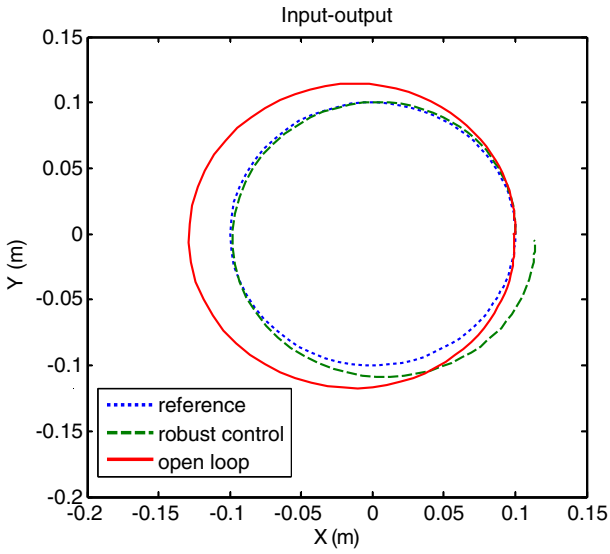

Fig. 9 Comparison of tracking of the uncertain system under ordinary feedback linearization control system and robust one

The red continues line shows the tracking of uncertain system under ordinary feedback linearization control system and the green dotted line shows the same result for the system equipped with robust controller. It is obvious that the summation of tracking error and also the maximum amount of error are considerably (more than 60%) decreased in the system equipped with robust control system.

5 DLCC Formulation for a Predefined Trajectory

5.1 Derivation of Formulation

The main goal of this paper is defining the DLCC of the robot based on saturated torque of the motors and allowable error bounds. According to [5] for a system that there is a linear relation between the applied torque by the motors and the mass of the end-effector, it is possible to use the following algorithm to determine the DLCC of the robot:

1) Determining the predefined trajectory.
2) Deriving dynamic equations of the system.
3) Forming the state space and imposing the control algorithm.
4) Dividing the path into n elements and assuming a prediction for DLCC.
5) Modeling and simulating the system along the path for both full-load and no-load end-effector.
6) Calculating the torque coefficient and accuracy coefficient and determining the DLCC based on factors calculated by Eq. 37.
7) Comparing the result with the predicted guess:
   a) Averaging between the result and the predicted guess in the case that there is a difference.
   b) Defining the result as the DLCC of the robot in the case that these values are the same with a good accuracy.
8) Iterating the algorithm till achieving the stage (7-b).

The coefficient of torque should be determined as below:

$$if\,(\tau_e)_i \geq 0 \rightarrow (C_a)_i = \frac{\tau_i^+}{(\tau_e)_i - (\tau_n)_i};\ \tau_i^+ = \left(U^+\right)_i - (\tau_e)_i,\ U^+ = k_1 - k_2\dot{q}$$

$$if\,(\tau_e)_i \leq 0 \rightarrow (C_a)_i = \frac{\tau_i^-}{(\tau_e)_i - (\tau_n)_i};\ \tau_i^- = \left(U^-\right)_i - (\tau_e)_i,\ U^- = -k_1 - k_2\dot{q} \quad (37)$$

where $k_2 = \tau_s/\omega_n$, $k_1 = \tau_s$, τ_s is the stall torque of the motors, ω_n is the free running angular velocity of the motors, $(\tau_e)_i$ is the torque of the motors calculated by dynamic equations of the full-load system for the ith element of the path, $(\tau_n)_i$ is the same amount for no-load system and τ_i^+, τ_i^- are the upper and lower bounds of the motors torque. So the DLCC of each motor can be determined as:

$$C_a = \min\{abs\,(C_a)\};\ i = 1, 2, \ldots, n \quad (38)$$

This coefficient should be calculated for all of the motors of the system and the minimum of them should be applied in order to determining the DLCC:

$$C = \min\left\{(C_a)_j\right\};\ j = 1, 2, \ldots, 6 \Rightarrow m_{load} = C * m_e \quad (39)$$

It should be considered that for calculating the DLCC of a robot which is under the control of a closed loop controller, there is no need to consider the accuracy coefficient because in such systems the deviation of the end-effector due to increasing the load is improved by the aid of controller by increasing the required motors torque that should be exerted by the motors and so there is no change in the accuracy of the tracking by increasing the load of the end-effector. In fact both of these two factors can be combined into the first one, torque accuracy, and it should just be considered that the amount of the motors torque do not violate the allowable bounds.

As it was mentioned, the linear relation between the motors torque and the load is a required factor for using the algorithm explained for DLCC, it can be seen that the same situation is also exists for a cable robot, Eq. 2 in the form of operator becomes:

$$\dot{X} = DX;\ \ddot{X} = D^2X \Rightarrow rmD^2X + S(X)\,J(\partial\beta/\partial X)\,D^2X + S(X)\left(J\frac{d}{dt}(\partial\beta/\partial X) + C(\partial\beta/\partial X)\right)DX = S(X)\,\tau \tag{40}$$

Since there is no parameter that is a function of m except itself, this equation can be rewritten in the following form:

$$\begin{aligned} S(X)\,\tau &= C * m + B;\\ C &= rD^2X;\\ B &= S(X)\,J(\partial\beta/\partial X)\,D^2X + S(X)\left(J\frac{d}{dt}(\partial\beta/\partial X) + C(\partial\beta/\partial x)\right)DX \end{aligned} \tag{41}$$

This shows a kind of linearity between torque and mass.

5.2 Simulation of the DLCC Algorithm

Using the mentioned algorithm, the end-effector's load is changed by trial and error method in a circular loop as described in the previous section till the first motor torque profile is saturated and becomes tangent to the allowable torque bounds (Table 7).

5.2.1 Planar DLCC Simulation

Consider the above characteristics for the planar system described in the previous sections:

Simulation test is performed for the circular trajectory as described in the simulation section; applying the mentioned algorithm results in about 2.2 kg load

Table 7 DLCC characteristics of planar model

Name	Symbol	Value	Unit
Mass of the end-effector	m_n	1	kg
Predicted guess of the load	m_l	2	kg
Maximum allowable error bound of tracking	R	0.01	m
Free running angular velocity of the motors	ω_n	1,000	rpm
Stall torque of the motors	τ_s	5	N.m

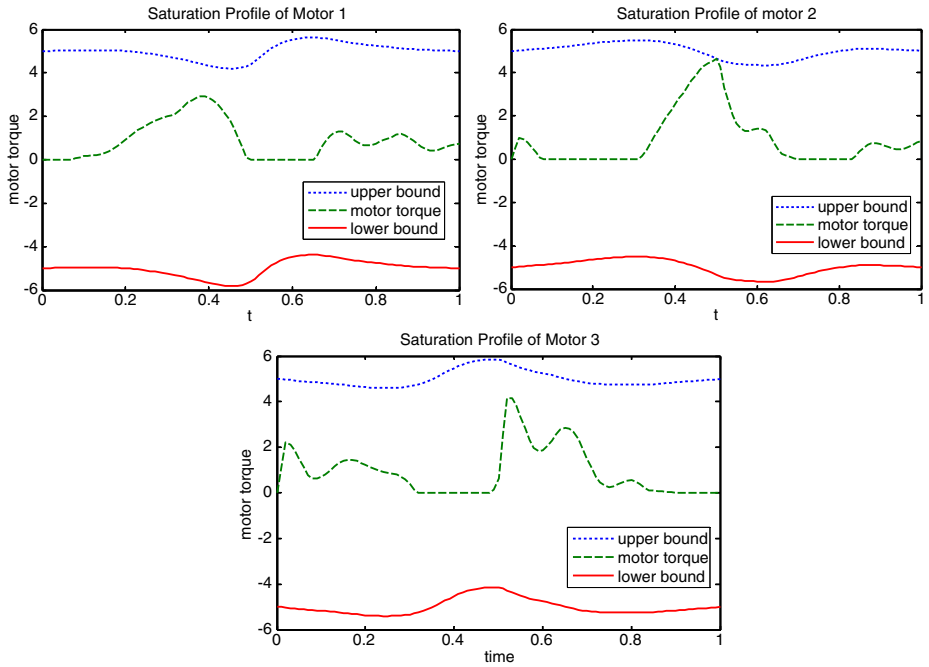

Fig. 10 Saturation profiles of motors torque of planar simulation

capacity which causes the first saturation in the second motor as is shown in Figs. 10 and 11.

It can be seen that the profile of the trajectory passed by the end-effector is not violated compared to its allowable bounds because of the application of the controller: Fig. 11.

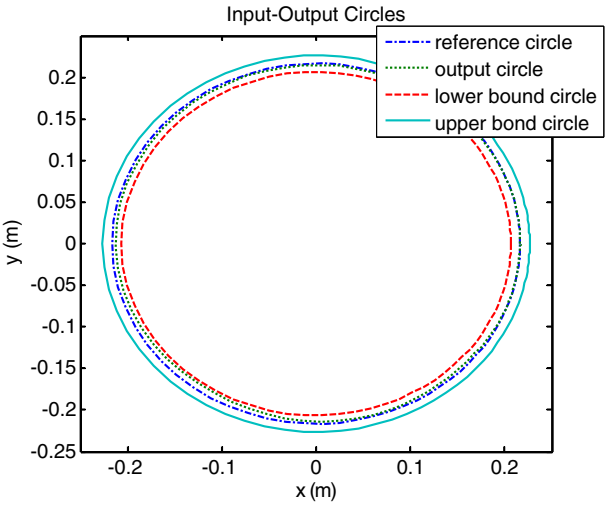

Fig. 11 Input-output paths of planar DLCC simulation

5.2.2 Spatial DLCC Simulation

In a similar way consider the following values for the parameters of Table 7 for the described spatial system: Table 8.

Same algorithm results in about 2.56 kg load capacity which causes the first saturation at the second motor as is shown in Figs. 12 and 13.

Table 8 DLCC characteristics of spatial model

Name	Symbol	Value	Unit
Mass of the end-effector	m_n	10	kg
Predicted guess of the load	m_l	5	kg
Maximum allowable error bound of tracking	R	0.01	m
Free running angular velocity of the motors	ω_n	1,000	rpm
Stall torque of the motors	τ_s	10	N.m

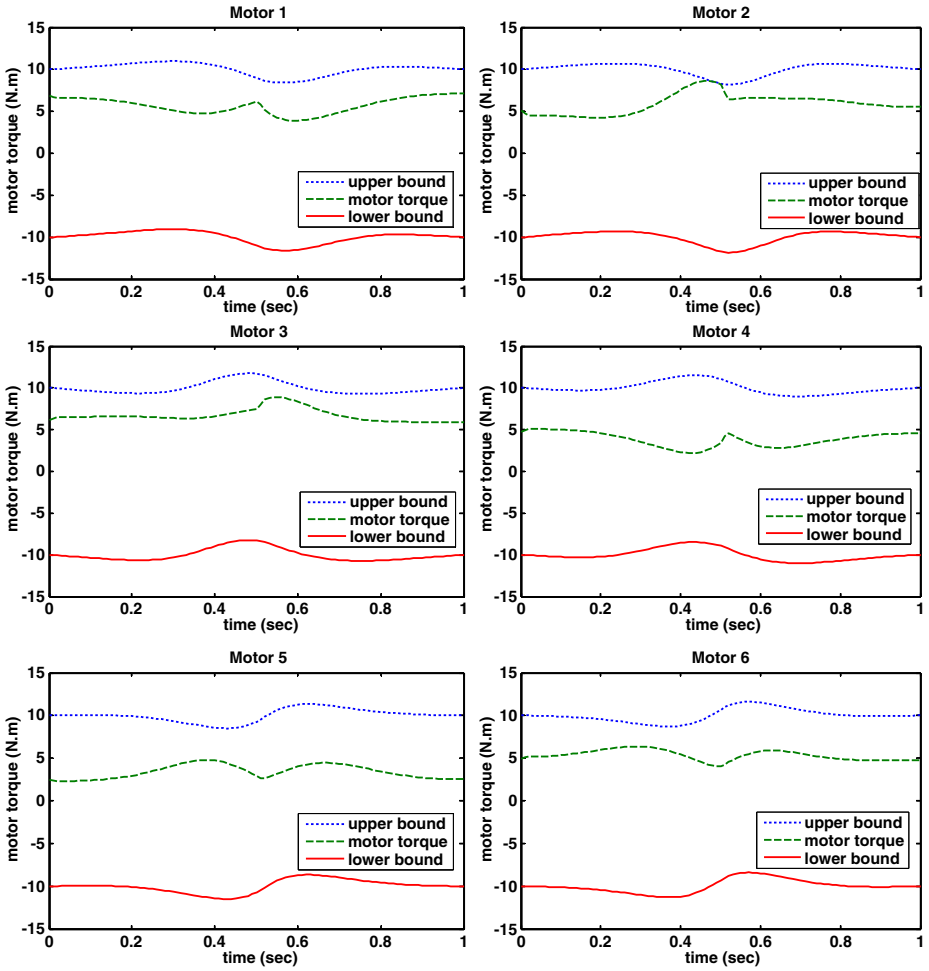

Fig. 12 Saturation profiles of motors torque of spatial simulation

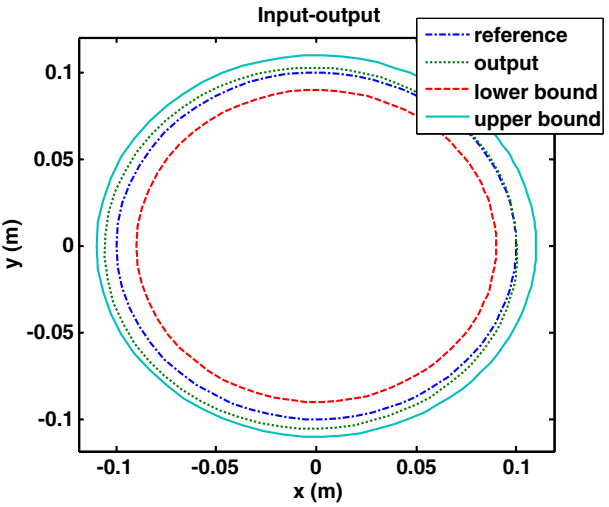

Fig. 13 Input-output path of spatial DLCC simulation

5.2.3 Flexible Joints DLCC Simulation

The second constrain is verified first. Circular path and other DOFs are shown in Fig. 14:

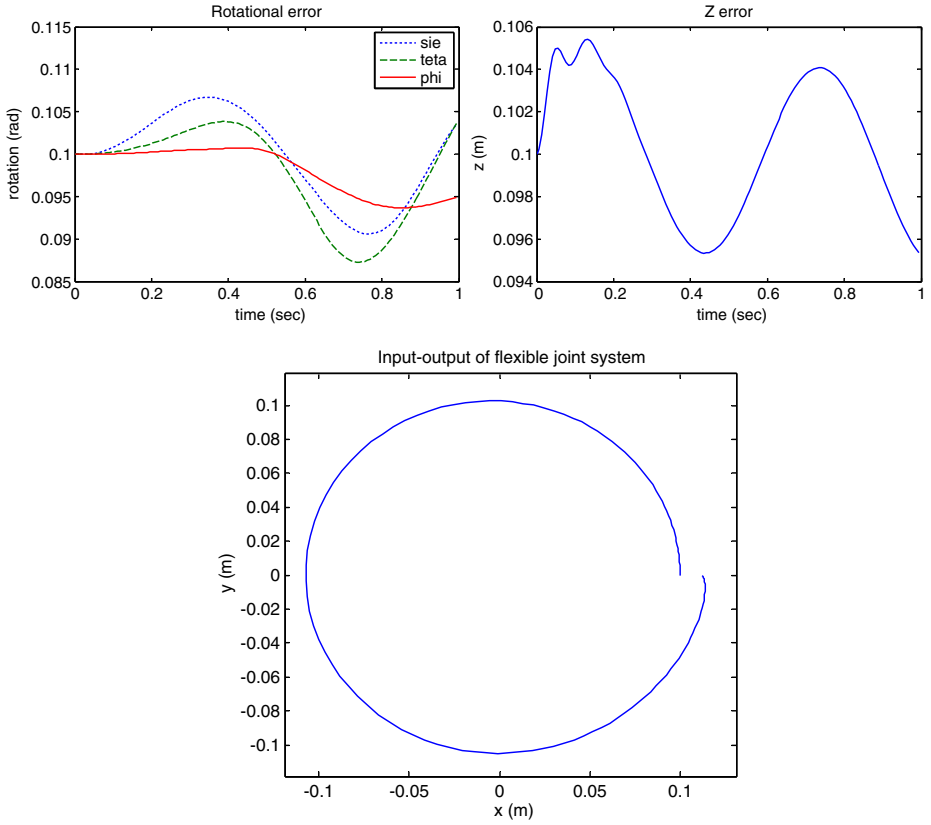

Fig. 14 Circular path and other DOF errors of flexible joint spatial DLCC simulation

It can be seen that responses are stable and do not violate the allowable defined bound ($R = 0.01$ m). So the next step is to study the torque saturation profile for each case. Consider the following characteristics for the motors with previous mass for the end-effector (Table 9).

The robot with elasticity coefficient equal to 3 N/rad results in 1.4 kg load capacity which is considerably less than rigid result (2.56 kg) and causes the first saturation in the second motor (Fig. 15).

Table 9 Motor specifications of flexible joints robot for DLCC

Name	Symbol	Value	Unit
Maximum allowable error bound of tracking	R	0.01	m
Free running Angular velocity of the motors	ω_n	1,000	rpm
Stall torque of the motors	τ_s	10	N.m

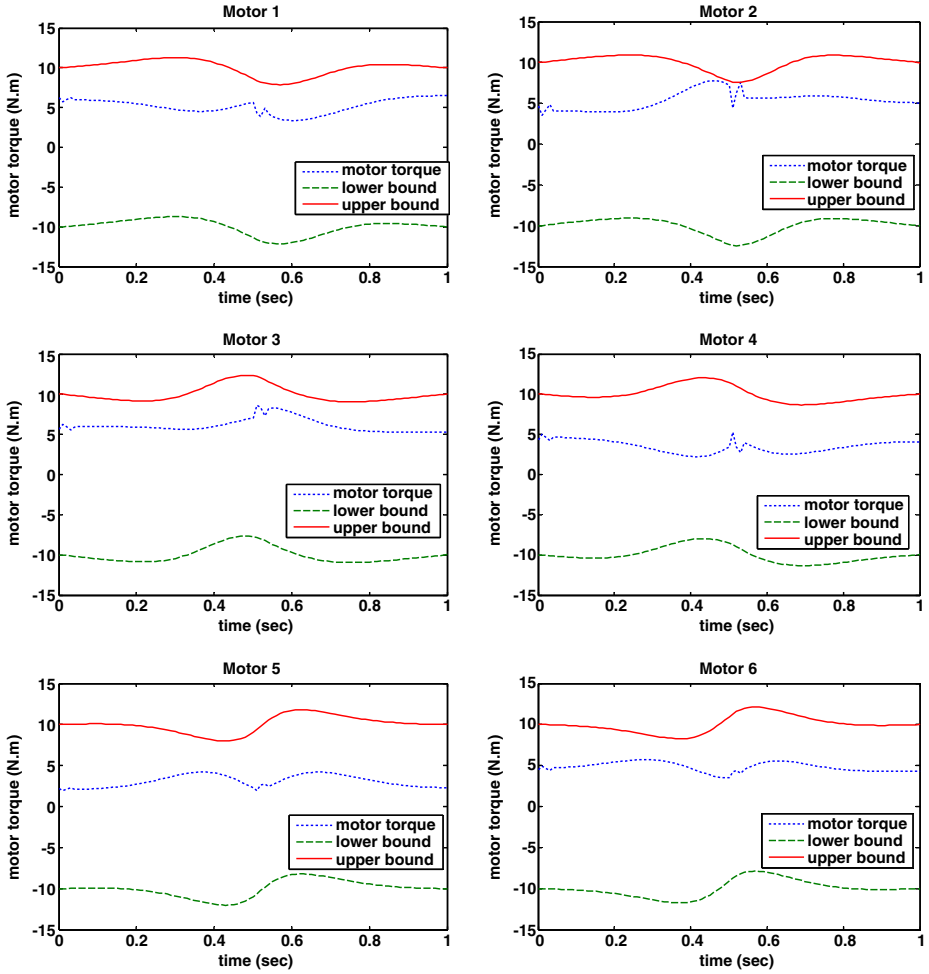

Fig. 15 Saturation torque profiles for elastic joint cable robot

6 Conclusion

Cable robots are controlled using feedback linearization control method. Required motors torque to control the end-effector within a predefined trajectory was calculated not only for rigid robots but also for elastic joints case. Also comparison between them was done by the aid of resulted profiles. Considering the risk of instability of uncontrolled states in flexible robot system caused by the noises or parametric uncertainties, robust control formulation was driven and added to the control system and its positive effect on path tracking was shown. An iterative algorithm for calculating the dynamic load carrying capacity (DLCC) of cable robot as a practical parameter of a robot was presented for a closed loop system considering motor torque and accuracy constrains. Torque saturation profiles and DLCC values were calculated. Simulation results proved the effectiveness of the designed controller and also showed that elasticity in the cable robots can change the torque profile during input changes. It was seen that these changes of required motors torque cause some decrease in the DLCC of the robot for flexible joints which was about 30% in the mentioned example. Also it was shown that existence of any kind of uncertainties can affect on the flexible robot tracking which can be improved more than 60% by adding the robust controller to the control system. Finally results show some improvements compared to open loop versions for tracking as well as DLCC.

References

1. Albus, J.S., Bostelman, R., Dagalakis, N.G.: The NIST Robocrane. J. Robot. Syst. **10**(5), 709–724 (1993)
2. Williams ll R.L., Gallina, P., Rossi, A.: Planar cable direct driven robots; Part 1: kinematics and statics. In: ASME Design Technical Conferences, 27th Design Automation Conference, vol. 2, pp. 1233–1240 (2001)
3. Korayem, M.H., Bamdad, M.: Dynamic load carrying capacity of cable-suspended parallel manipulators. Int. J. AMT. **44**(7–8), 1133–1143 (2009)
4. Alp, A.B., Agrawal, S.K.: Cable Suspended Robots: Design, Planning and Control. Department of Mechanical Engineering, University of Delaware (2001)
5. Korayem, M.H., Davarpanah, F., Gariblu, H.: Load carrying capacity of flexible joint manipulator with feedback linearization. Int. J. AMT. **29**(3–4), 389–397 (2006)
6. Korayem, M.H., Firouzi, S.: Dynamic load carrying capacity of mobile-base flexible-link manipulators: feedback linearization control approach. Proc. IEEE Int. Conf. Robot. Biomimetics. 2172–2177 (2007)
7. Dolorez, F.J., Russ, H.: Planar Direct Driven Robot. College of Engineering and Technology of Ohio University (2003)
8. Yamamoto, M., Yanai, N., Mohri, A.: Trajectory control of incompletely restrained parallel-wire-suspended mechanism based on inverse dynamics. IEEE Trans. Robot. **20**(5), 840–850 (2004)
9. Spong, M.W.: Modeling and Control of Elastic Joint Robots. Coordinate Science Lab., University of Illinois at Urbana Champaign (1987)
10. Chen, G.: Exact Closed-form Optimal Solution for Constrained Trajectory Control of Single-link Flexible Joint Manipulator. Department of Electrical Engineering, University of Houston, Texas (1990)
11. Zhang, Y., Agrawal, S.K., Piovoso, M.J.: Coupled dynamics of flexible cables and rigid end-effector for a cable suspended robot. American Control Conference (2006)
12. Shiang, W.J., Cannon, D., Gorman, J.: Dynamic analysis of the cable array robotic crane. In: IEEE International Conference on Robotics & Automation, Detroit, vol. 4, 2495–2500 (1999)

13. Korayem, M.H., Bamdad, M.: Workspace analysis of cable-suspended robots with elastic cable. In: Proc. of the IEEE International Conference on Robotics and Biomimetics, ROBIO, Sanya, China, vol. 5, pp. 1942–1947 (2007)
14. Baicu, C.F., Rahn, C.D., Nibali, B.D.: Active Boundary Control of Elastic Cables. Theory and Experiment. Department of Mechanical Engineering, Clemson University, ScienceDirect (2002)
15. Williams, R.L.: Planner cable suspended haptic interface: design for wrench exertion. ASME Des. Tech. Conf. **35**, 203–219 (1999)
16. So-Ryeok Oh: Cable Suspended Robots: Control Approaches and Applications. Ph.D. Thesis, University of Delaware (2006)
17. Korayem, M.H., Bamdad, M., Bayat, S.: Optimal trajectory planning with dynamic load carrying capacity of cable-suspended manipulator. In: IEEE International Symposium Mechatronics and its Applications, ISMA, pp. 1–6 (2009)